Solubilization of Decane into Gemini Surfactant with a Modified Jeffamine Backbone: Design of Hierarchical Porous Silica

A. May-Masnou [a,b,c], A. Pasc[a,b], M.J. Stébé[a,b], J.M. Gutiérrez[c], M. Porras[c] and J.L. Blin[a,b*]

[a]: Université de Lorraine/CNRS, SRSMC, UMR7565, F-54506 Vandoeuvre-lès-Nancy cedex, France

[b]: CNRS, UMR7565, F-54506 Vandoeuvre-lès-Nancy cedex, France

[c]: Departament d'Enginyeria Química, Facultat de Química, Universitat de Barcelona, Martí i Franquès 1-11, 08028, Barcelona, Catalunya, Spain

*** Corresponding author : Pr. Jean-Luc Blin**
Université de Lorraine
UMR CNRS 7565 SRSMC
Faculté des sciences et technologies
BP 70239
54506 Vandoeuvre les Nancy cedex
Tel : + 33 3 83 68 43 70
Fax : + 33 3 83 68 43 44
e-mail : Jean-Luc.Blin@univ-lorraine.fr

Published in: Microporous and Mesoporus Materials, Volume 169, 2013, Pages 235-241

Abstract

Herein, we have investigated the solubilization of decane into a novel nonionic gemini surfactant, myristoyl-end capped Jeffamine, synthesized from a polyoxyalkyleneamine (ED900). Starting from this system, porous silica materials have been prepared. Performing the hydrothermal treatment at low temperature, a slight increase of the mesopore diameter is observed in the presence of decane. Increasing the temperature of the hydrothermal treatment, no swelling effect of decane is detected. By contrast, the pore diameter decreases but better mesopore homogeneity and a larger wall thickness are obtained. At high decane concentration the new myristoyl-end capped Jeffamine/decane/water system forms oil-in-water emulsions, which are used as template for the formation of hierarchical porous silica materials.

Keywords: modified Jeffamine; phase diagram; oil solubilization; emulsion-templating; hierarchical silica

Published in: Microporous and Mesoporus Materials, Volume 169, 2013, Pages 235-241

1. Introduction

Porous inorganic materials with tailorable, hierarchical and uniform pore structures, in the meso- and macro-range, are emerging and constituting themselves as an important class of solid materials in a wide variety of applications such as ion-exchange resins [1], catalyst supports [2], sensors [3] and tissue engineering [4]. Thanks to the textural mesopores associated with intrinsic interconnected pore systems of macrostructures, these materials should efficiently transport guest species to framework binding sites. The macropore network can be created by different ways. A general procedure requires the use of latex spheres as templating agents [5-7]. Colloidal latex spheres, all having the same diameter, first aggregate in a regular lattice, then the inorganic precursors and surfactant (or copolymer) micellar solution are allowed to infiltrate the spaces between the spheres, and then condensation and crystallization takes place. The removal of the surfactant and colloidal latex spheres, by either high-temperature calcination or solvent extraction, leads to the formation of three-dimensional ordered meso–macroporous materials (3DOM) [5]. Tiddy and co-workers [6,7] synthesized a series of hierarchically ordered porous silica composites with ordering on three different scales of pore size by using latex spheres and triblock copolymers (Pluronic F127 and P123) as template in the presence of cosurfactant (n-alcohol) in an acidic medium. The silica materials consist of three-dimensional ordered macropores (200 – 800 nm) with interconnecting, uniform-sized (70 – 130 nm) windows, and the walls of these macropores consist of mesostructured pores (3– 8 nm), as well as a significant microporosity (< 2 nm), presenting a macro-meso-microporous structure with a three-dimensional interconnectivity. In a paper dealing with solid lipid nanoparticles (SLN) templating of alveolar macroporous silica beads [8,9], we have demonstrated that SLN, prepared from the solvent injection technique, can also be used to generate the macropore network. Finally, materials with a macroporous structure can be formed through the emulsion templating process [10-20]. This pathway has

been used to produce macroporous titania, silica and zirconia with pore sizes from 50 nm to several micrometres [10]. Because the emulsion drops are deformable, macroscopic samples are able to accommodate stresses that arise during gelation and shrinkage. Samples prepared using rigid spheres, by contrast, tend to break into small pieces that are seldom larger than a few hundred micrometres. In addition, emulsification conditions can be adjusted to produce droplets with different mean sizes which are typically in the micrometre range. Moreover, this can be done to a large extent independently of the self-assembling block copolymer species used to direct the structure of the mesopores. This allows a control of macro- and mesopore dimensions, so the final pore structures can be tailored to different diffusion and reaction conditions [21]. Introduction of mesoporosity in a macroporous structure has been reported by a surfactant emulsion-mediated synthesis. Tiddy and co-workers [21, 22] have used this approach to achieve the room-temperature synthesis of a macro-mesoporous silica material. The formation of macro-cellular foams is explained based on a natural phenomenon of oil-in-water emulsion known as “creaming” which is the migration of the dispersed phase of an emulsion, under the influence of buoyancy. This synthesis was carried out using cetyltrimethylammonium bromide (CTAB) as surfactant and trimethylbenzene as oil. Cooper and co-workers reported the synthesis of porous emulsion-templated polymer/silica composite beads by sedimentation polymerization of a high internal phase emulsion (HIPE) [12]. High surface area silica beads with an average diameter of 1.3 mm, high pore volume of 5.7 cm^3g^{-1} and interconnected macropore structure were obtained by calcination of the composite structures. The HIPE structure was retained in the silica beads and the material had high surface area (422 m^2g^{-1}). Indeed, this semi-continuous synthetic procedure could be scaled up to allow the synthesis of significant quantities of beaded materials with a narrow particle size distribution. Carn and co-workers [23] prepared hierarchical inorganic porous monoliths with a double template, *i.e.* direct emulsion at the macroscale and micellar solution at the

mesoscale. The monolithic materials had typical polymerized high internal phase emulsion (poly-HIPE)-type interconnected macroporous network with polydisperse cell and window sizes within the micrometre range. These materials show interconnected macroporosity with disordered structures. The mesopores size varies from 1.2 to 4.0 nm. Recently, we have reported the preparation of ordered mesoporous materials from a novel nonionic gemini surfactant, myristoyl-end capped Jeffamine, synthesized from a polyoxyalkyleneamine (ED900) [24]. Here, we have investigated the effect of decane solubilization in this new system in relation with the design of hierarchical porous silica through the emulsion templating pathway.

2. Materials and methods

H_2N-$(OC_3H_7)_3(OC_2H_4)_{12.5}(OC_3H_7)_3NH_2$ (trade name Jeffamine **ED900** (XTJ-501)) was supplied by Huntsman Corporation. It is based on a polyether $(PO)_x$-$(EO)_y$-$(PO)_z$ backbone containing primary amino groups attached at both ends and it is presented as a transparent viscous liquid at ambient temperature. Myristic acid, decane and tetramethoxysilane (TMOS), used as silica source, were purchased from Sigma-Aldrich. Deionized water was obtained using a Milli-Q water purification system. Jeffamine ED900 was modified according to the procedure we have previously reported [24].

2.1 ED900Myr/decane/water phase diagram determination

The phase diagram has been established by preparing samples over the whole range of surfactant/water compositions. The required amounts of surfactant, decane and water were introduced into well-closed glass vials to avoid evaporation. The mixture was homogenized using a Vortex stirrer and samples were placed in a thermostatic bath at 20 °C until the equilibrium was reached. The different phases were identified by visual inspection with a

polarizing light microscope (Olympus BX 50). The boundary lines of the liquid crystal domains were evidenced by Small Angle X–ray Scattering (SAXS) experiments.

2.2 Porous material preparation

The materials were prepared from a 5 wt % micellar solution at neutral conditions. Decane, which was incorporated under stirring, varied from 1 to 85 wt %. The other steps are the same than those used for the preparation of the materials in the absence of decane [24].

2.3 Characterization of porous materials

SAXS measurements were carried out using SAXSess mc2 (Anton Paar) apparatus. It is attached to a ID 3003 laboratory X-Ray generator (General Electric), equipped with a sealed X-ray tube (PANalytical, $\lambda_{Cu\ (K\alpha)}$ = 0.1542 nm) operating at 40 kV and 50 mA. A multilayer mirror and a block collimator provide a monochromatic primary beam. A translucent beam stop allows the measurement of an attenuated primary beam at q = 0. Porous materials are introduced into a powder cell whereas liquid crystals are placed in a paste cell. Samples are placed inside an evacuated chamber. Acquisition times are typically in the range of 1 to 5 minutes. Scattering of X-ray beam is recorded by a CCD detector (Princeton Instruments, 2084 x 2084 pixels array with 24 x 24 µm² pixel size) in the q range 0.09 to 5 nm^{-1}. The detector is placed at 309 mm from the sample holder. Scattering data, obtained with a slit collimation, contain instrumental smearing. Therefore, the beam profile has been determined and used for the desmearing of the scattering data. All data were corrected for the background scattering from the empty cells. Samples for transmission electron microscopy (TEM) analysis were prepared by dispersing some material in ethanol. Afterwards a drop of this dispersion was placed on a holey carbon coated copper grid. A Philips CM20 microscope, operated at an accelerating voltage of 200 kV, was used to record the images. Scanning electron microscopy (SEM) was carried out with a HITACHI S-2500 at 15 keV. N_2 adsorption and desorption isotherms were determined on a Micromeritics TRISTAR 3000

sorptometer at –196 °C. The pore diameter and the pore size distribution were determined by the BJH (Barret, Joyner, Halenda) [25] method applied to the adsorption branch of the isotherm.

3. Results and discussion

3.1 The myristoyl-end capped Jeffamine (ED900Myr)/decane/ water ternary system

Figure 1 shows the phase diagram of the ED900Myr/decane/water system at 20°C. At this temperature, below 13 wt % of ED900Myr less than 1 wt % of decane can be incorporated in the micelles. If the decane loading is increased the solution becomes turbid, a Winsor I system is obtained. The lower phase is composed of the swollen micelles, whereas the oil excess constitutes the upper phase. Increasing the surfactant concentration between 13 and 45 wt %, the micelles can accommodate up to 8 wt % of decane. It should be noted that between 35 and 42 wt % of ED900Myr in water, a micellar cubic phase is formed between 3 and 15 wt % of oil. The existence range of the cubic structure is limited. When the weight percent of surfactant is increased from 47 to 72 wt %, an optically anisotropic phase is detected. The fan-shape texture observed by optical microscopy with polarized light is characteristic of the defects of the direct hexagonal H_1 phase. The hexagonal symmetry is confirmed by SAXS measurements. The surfactant range composition belonging to H_1 is progressively reduced as the decane loading is increased. Indeed, as it can be seen in Figure 1, the $C_{10}H_{22}$ incorporation in the hexagonal phase is strongly dependent on the ED900Myr/water ratio (noted R): the amount of decane accommodated in H_1 varies from 3 to 20 wt % when R is changed from 1 to 2.31. If the surfactant concentration is further increased (> 75 wt %) the gel phase (L_β) appears.

On the other hand, in the oil-rich corner of the phase diagram, oil-in-water emulsions and highly-concentrated emulsions (decane content higher than 74 wt %) are formed. It should be

noted that the stability of these emulsions is enough to prepare the porous silica materials. Based on geometrical considerations [26], the structural parameters of the hexagonal liquid crystal phases have been determined. Indeed, the hexagonal structure is characterized by three Bragg reflections whose positions are in the ratio 1:√3:2 and the value of $d_{100,}$ given by the first reflection is related to the radius of the hydrophobic core (R_H) (alkyl chains + PO units) by the following relation (1):

$$\frac{V_B + \beta V_O}{V_S + \alpha V_W + \beta V_O} = \frac{\sqrt{3}\pi R_H^2}{2d_{100}^2} \qquad (1)$$

where α and β are the numbers of water and oil molecules respectively per surfactant molecule. V_B is the molar volume of the hydrophobic part of surfactant, which is calculated from the molar volumes of the two myristoyl chains and of the six PO units (V_B = 935 cm^3/mol). V_S, V_W and V_O correspond to the molar volumes of the surfactant (V_S = 1392 cm^3/mol), water (V_W = 18 cm^3/mol) and oil (V_O = 194 cm^3/mol). The cross sectional area (S) per surfactant molecule can then be deduced from the following relation (2):

$$S = \frac{2(V_B + \beta Vo)}{N\ R_H} \qquad (2)$$

where N is the Avogadro constant.

Figure 2 depicts the variation of the structural parameters, together with the value of the d_{100} reflection, with β, for different ED900Myr/water ratios (R). For a given R, as shown in Figure 2A, an increase in the d-spacing and, thus, in the cell parameter is noted with increasing the oil content. Incorporation of decane also leads to an increase in R_H (Fig. 2B), but in the mean time the value of the cross sectional area decreases (Fig. 2C). For example for R = 2.31, R_H varies from 2.0 to 3.5 nm meanwhile S drops from 1.53 to 1.33 nm^2 when β is changed from 0 to 2.39. According to previous work [27-29], when oil is added, it either penetrates into the amphiphilic film (penetration effect) or forms a core (swelling effect). Both effects can also simultaneously occur. In a paper dealing with the effect of oil on the

structure of liquid crystals in polyoxyethylene dodecylether-water systems, Kunieda et *al.*[30,31] reported that saturated hydrocarbons such as decane favor a swelling of the hexagonal structure core cylinders, whereas aromatic hydrocarbons such as m-xylene tend to penetrate the surfactant palisade layer. In addition, the solubilization of aromatics and aliphatic solubilizates in block copolymer micelles has been investigated in detail by Nagaraján et *al.* [32-34]. The authors have shown that both kinds of compounds are incorporated in the hydrophobic micellar core and that large solublization capacities and high selectivity for aromatics over aliphatics are obtained in block copolymer micelles compared with conventional low-molecular-weight surfactant micelles. The molecular structure of ED900Myr is similar to the one of the block copolymers, so taking into account all of these considerations and the increase of R_H with β for a given ED900Myr/water ratio, we can assume that in the H_1 phase of the E900Myr/decane/water system decane is entrapped in the core of the rods, so swelling would be the predominant effect, whereas the penetration of decane molecules between the hydrophobic chains is limited. Actually, Figure 2C indicates that upon the addition of decane the cross sectional area decreases as a function of β. A similar behavior has been noted by Lindman et *al.* [35] for the solubilization of p-xylene in the direct liquid crystal phases in poloxamer block copolymer based systems. In spite this variation, the authors conclude that xylene is located in the core of the oil-in-water microdomains and that no xylene is expected to partition at the polar/apolar interface. In our study the decrease of S indicates that the formation of an oil core occurs while the order of the polypropylene chains, which are folded in the ED900Myr/water binary system [24], is increased. As a consequence, in the hexagonal phase the amphiphilic molecules stretch and stiffen as decane is solubilized, involving a further increase of the hydrophobic radius.

3.2. Silica porous materials

Once the phase diagram was investigated and the liquid crystal structural parameters were evaluated, this new surfactant-based system was used for the preparation of silica porous materials. First the hydrothermal treatment has been performed at 50 °C during 44 hours. As a matter of fact we have shown that under these conditions the materials synthesized without oil exhibit a hexagonal pore ordering [24]. Upon addition of decane the hexagonal structure is kept as far the concentration of oil remains lower than 10 wt % (Fig. 3Ab-c). The position of the first peak varies from 5.1 to 5.4 nm when the oil loading is increased from 0 to 5 wt %. When the decane amount reaches 10 wt %, the first peak is strongly shifted toward lower q values, the d-spacing is changed from 5.4 to 6.5 nm (Fig. 3Ad). However, the peaks become broader, their intensity decreases and the 110 and 200 reflections are not well resolved. So, the organization of the channel array has begun. According to the IUPAC classification [36] a type IV isotherm with a *H1* hysteresis loop is obtained for the samples prepared with a concentration of decane lower than 10 wt % (Fig. 3B). A hysteresis loop similar to *H2* type, in which the desorption branch is steep but adsorption branch is more or less sloping, corresponds to samples prepared with 10 wt % of decane. This change of hysteresis loop is in agreement with the disorganization of the materials evidenced by SAXS. In fact, the *H2* type hysteresis loop is often encountered for disordered materials with a wormhole structure. The maximum of the pore size distribution is shifted from 3.9 to 4.4 nm when the amount of oil is varied from 0 to 10 wt % (Fig. 3C), indicating that in this range of concentration decane acts as an expander. The maximum of the pore size distribution of the material prepared with a decane loading equal to 10 wt % shows a low dV/dD value (Fig. 3C), reflecting the disorganization of the mesopore network. The results reported above indicate that decane can be used as oil to slightly swell the ordered mesopore of the materials prepared from the new

ED900Myr based system. However, in the first part of this paper, we have evidenced that for 5 wt % of the myristoyl-end capped Jeffamine only a very small quantity (≈ 1 wt %) of decane can be incorporated into the micelles (L_1) of ED900Myr in water, thus we cannot consider a swelling effect of the micelle core to explain the pore size expansion upon the addition of decane. Nevertheless, when TMOS is added to the surfactant, water and oil mixture, a hexagonal hybrid mesophase, whose features are analogous to the H_1 liquid crystal is formed through the CTM-type mechanism and it should be reminded that decane can swell the rod of the hexagonal liquid crystal phase. So concerning the swelling mechanism of mesoporous materials we propose that decane can be incorporated in this surfactant-silica hybrid hexagonal mesophase involving by this way the slight pore size expansion. It should be noted that a small uptake in the mesopore size was also observed for SBA-15 when alkanes are used as expanders. It is reported for SBA-15, prepared from P123 surfactant that the pore size increases when the chain length of alkane decreases in a series from decane to pentane [37, 38]. One way to modify the value of the pore diameter consists in changing the conditions of the hydrothermal treatment [39-43]. The latter has been performed during 24 hours at 80 °C and in that case the decane loading was increased up to 85 wt % to study the characteristics of the materials in the whole range of decane concentrations, from diluted to highly-concentrated emulsions. The SAXS pattern of the material prepared in the absence of oil exhibits a broad reflexion at 5.1 nm (Fig. 4Aa), indicating the arrangement of the channels into a wormhole-like structure. Until 3 wt % of oil no change is observed (Fig. 4Ab), but between 3 and 5 wt %, there is a large step in the d-spacing, which increases from 5.4 to 6.3 nm (Fig. 4Ac) and becomes less sharp. From 5 to 10 wt %, the peak moves from 6.3 to 7.4 nm and a second reflection peak, less resolved, is observed (Fig. 4Ad). Beyond this concentration the position of the broad peak remains almost constant at 7.6 nm (Fig. 4Ae-i). The detection of the Bragg reflections indicates that the mesopores are still present and that a

transition from a wormhole-like to a more ordered structure occurs even if the hexagonal arrangement is not reached. A type IV isotherm with a H1 hystheresis loop is obtained for the samples prepared with a decane concentration lower than 5 wt % (Fig. 4B). The mesopore diameter is more or less constant around 7.0 nm (Fig. 5A), which is similar to the value obtained for the materials prepared without oil. So, in this range of concentration, no swelling effect of decane occurs. Upon the further addition of decane a change of the shape of the isotherms is observed (Fig. 4B). At high relative pressures (beyond $p/p_0 = 0.9$), the adsorbed volume of nitrogen increases significantly instead of remaining constant due to saturation and the isotherm becomes a combination between type IV and type II . Contrary to what one can expect regarding the evolution of the d-spacing, the value of the relative pressure at which the capillary condensation occurs decreases with the decane concentration. Since the p/p_0 position of the inflection point is related to the pore diameter according to Kelvin's equation, this observation suggests that the pore diameter decreases when oil is added. This unexpected behavior is further confirmed by the evolution of the mean pore diameter (Fig. 5A), which falls to 5.9 nm when the decane concentration reaches 5 wt %; after that it slowly decreases from 5.9 to 4.4 nm when the amount of decane varies from 5 to 85 wt %. We can also observe from Figure 4B that the mesopore size distribution becomes narrower. This means that upon the addition of decane an enhancement in the homogeneity of the mesopores occurs. Whatever the loading, the specific surface area is rather high. However, its value slowly decreases with the incorporation of oil (Fig. 5B). In these conditions decane does not act as a swelling agent. Since such a behavior is not observed when the hydrothermal treatment is performed at lower temperature, one can assume that the combination of both the addition of decane and the increase of temperature involves a reorganization of the ED900Myr molecules in the micellar phase, which leads to the formation of surfactant aggregates with a smaller hydrophobic core, probably due to a change of the conformation of myristoyl chains and/or of

the PO units. As a matter of fact, the behavior of nonionic surfactant can be strongly modified by the presence of additives or by the temperature. The hydrolyzed TMOS interacts with these aggregates giving rise to the mesopore network. The modification of micelles in the presence of decane has been reported by Bao et *al.* to explain the synthesis of submicrometer-sized SBA-15 materials with highly ordered short-pore channels in the presence of large amounts of decane [44]. Decane can confine the formation of silica-doped micelles, resulting in a decrease of particle size and a change of the channel orientation. The authors have also reported that the addition of fluoride is needed to get a mesopore ordering. In the absence of NH_4F, disordered mesoporous silica are obtained even with large amounts of decane. Here, no fluoride has been added that can explain why no hexagonal mesopore ordering is obtained even if an improvement of the organization is detected. In addition, the value of the d-spacing, corresponding to the sum of the pore diameter and the thickness of the pore wall, remains almost constant between 5 and 85 wt % of decane (Fig. 5A). It can thus be inferred that the wall thickness increases upon the addition of decane. Figure 6 shows several representative scanning electron micrographs (SEM) and TEM images of the synthesized porous silica. While at low decane concentration the morphology of the particles can be described as agglomerates of cylinders (Fig. 6a,b), it appears that at high oil content (60-80 wt %) the ED900Myr/decane/water system provides a macroporous network (Fig. 6c-e). The presence of the macropores is also detected on the TEM images (Fig. 6f-i). The macropores are not well-ordered and the pore size is typically in the range of few hundred nanometers. Actually, when more and more decane is added oil-in-water emulsions are formed and the oil droplets template the formation of the macropore network. In such a mechanism, the silica source interacts with the surfactant surrounding the oil droplets creating casts of the morphological macropores. Performing the hydrothermal treatment at 100 °C during 24 hours and comparing the properties of the materials with the ones of the sample synthesized without oil, we observe

that the presence of decane also involves a decrease of the mesopore diameter and a narrowing of the pore size distribution. In that case when 5 wt % of decane are added the pore diameter decreases from 14.4 to 7.7 nm.

4. Conclusion

We have investigated the effect of the solubilization of decane into a novel nonionic gemini surfactant, myristoyl-end capped Jeffamine, synthesized from a polyoxyalkyleneamine (ED900). First, we have delimited the domains of the various phases and determined the structural parameters of the hexagonal liquid crystal phase. We have shown that below 13 wt % of ED900Myr in water, only a low quantity of oil can be incorporated in micelles (less than 1 wt %). Then the solubilization of decane in the micelles is increased and up to 8 wt % of the alkane can be incorporated into the micellar phase. Results also evidenced that in H_1 the cross sectional area decreases with the addition of decane. At the same time, the value of the hydrophobic radius (R_H), is raised. In addition, we have shown that at high content of oil, concentrated oil-in-water emulsions can be formulated. Mesoporous materials and meso-macroporous materials were then prepared from the ED900Myr/decane/water system. If the hydrothermal treatment is performed at 50 °C during 44 hours, decane acts as an expander. However the uptake of the pore diameter is rather low. Increasing the hydrothermal temperature to 80 °C during 24 hours, no swelling effect of decane is observed anymore. In contrary to what one could expect upon the addition of decane, the mean pore diameter decreases. In the same time the wall thickness is increased and a narrower pore size distribution is observed, meaning that more homogeneous mesopores are obtained. Under these conditions, the SAXS analysis reveals that a transition from wormhole-like to a more ordered structure occurs. The SEM and TEM experiments show that at high decane

Published in: Microporous and Mesoporus Materials, Volume 169, 2013, Pages 235-241

concentration the obtained oil-in-water emulsions can template the formation of hierarchical porous materials.

Acknowledgements :

Authors would like to thank Lionel Perdreau of Huntsman Surface Sciences (St Mihiel, France) for providing the Jeffamine surfactant. Authors would also like to thank Mélanie Emo for performing the X-ray measurements. Anna May would like to thank the Spanish MICINN for the financial support within the framework of the project number CTQ2008-06892-C03-03/PPQ.

References

[1] R.J. Wackeman, Z.G. Bhumgara, G. Akay, Chem. Eng. J. 70 (1998) 133.

[2] J.F. Brown, P. Krajnc, N.R. Cameron, Ind. Eng. Chem. Res. 44 (2005) 8565.

[3] M.S. Silverstein, H. Tai, A. Sergienko, Y. Lumelsky, S. Pavlovsky, Polymer 46 (2005) 6682.

[4] G. Akay, M.A. Birch, M.A. Bokhari, Biomaterials 25 (2004) 3991.

[5] B.T. Holland, C.F. Blanford A. Stein, Science 281 (1998) 538.

[6] T. Sen, G.J.T. Tiddy, J.L. Casci, M.W. Anderson, Angew. Chem. Int. Ed. 42 (2003) 4649.

[7] T. Sen, G.J.T. Tiddy, J.L. Casci, M.W. Anderson, Chem. Mater. 16 (2004) 2044.

[8] A. Pasc, J.L. Blin, M.J. Stébé, J. Ghanbaja, RSC Advances 1 (2011) 1204.

[9] R. Ravetti-Duran, J.L. Blin, M.J. Stébé, C. Castel, A. Pasc, J. Mater. Chem. 22 (2012) 21540.

[10] A. Imhof, D.J. Pine, Nature 389 (1997) 948.

[11] A. Imhof, D.J. Pine, Chem. Eng. Technol. 21 (1998) 8.

[12] H. Zhang, G.C. Hardy, M.J. Rosseinsky, A.I. Cooper, Adv. Mater. 15 (2003) 78.

[13] B.P. Binks, Adv. Mater. 14 (2002) 1824.

[14] J.L. Blin, R. Bleta, J. Ghanbaja, M.J. Stébé, Microporous and Mesoporous Mater. 94 (2006) 74.

[15] N. Du, J.L. Blin, M.J. Stébé, Colloids and surfaces A : Physicocehem. Eng. Aspects 357 (2010) 116.

[16] C. Oh, S.C. Chung, S.I. Shin, Y.C. Kim, S.S. Im, S.G. Oh, J. Colloids Interface Sci 254 (2002) 79.

[17] C. Zhao, E. Danish, N.R. Cameron, R. Kataku, J. Mater. Chem. 17 (2007) 2446.

[18] S. Zhang, J. Chen Polymer 48 (2007) 3021.

[19] J.L. Blin, J. Grignard, K. Zimny, M.J. Stébé, Colloids and surfaces A : Physicochem. Eng. Aspects 308 (2007) 71.

[20] R. Bleta, J.L. Blin, M.J. Stébé, J. Phys. Chem.B 110 (2006) 23547.

[21] T. Sen, G.J.T. Tiddy, J.L. Casci, M.W. Anderson, Chem. Commun. (2003) 2182.

[22] T. Sen, G.J.T. Tiddy, J.L. Casci, M.W. Anderson, Microporous and Mesoporous Mater. 78 (2005) 255.

[23] F. Carn, A. Colin, M.F. Achard, H. Deleuze, E. Sellier, M. Birot, R. Backov, J. Mater. Chem. 14 (2004) 1370.

[24] A. May, A. Pasc, M.J. Stébé, J.M. Gutiérrez, M. Porras, J.L. Blin, Langmuir 28 (2012) 9816.

[25] E.P. Barret, L.G. Joyner, P.P. Halenda, J. Am. Chem. Soc. 73 (1951) 37.

[26] M. Alibrahim, M.J. Stébé, G. Dupont, J.C. Ravey, J. Chim. Phys. 94 (1997) 1614.

[27] J.C. Ravey, M.J. Stébé in Surfactant in solution, K.L. Mittal, P. Bothorel; Eds : Vol. 79; Plenum : New York, (1989) p. 272.

[28] M.H. Ropers, M. J. Stébé, Langmuir 19 (2003) 3137

[29] J.L. Blin, M.J. Stébé, Microporous and Mesoporous Mater. 87 (2005) 67.

[30] H. Kunieda, K.Ozawa, K.L. Huang, J. Phys. Chem. B 102 (1998) 831.

[31] H. Kunieda, G. Umizu, K. Aramaki, J. Phys. Chem. B 104 (2000) 2005.

[32] R. Nagaraján, M. Barry, E. Ruckenstein, Langmuir 2 (1986) 210.

[33] R. Nagaraján, K. Ganesh, . Colloids Interface Sci 184 (1996) 489.

[34] R. Nagaraján, Colloids and surfaces B : Biointerfaces, 16 (1999) 55.

[35] P. Holmqvist, P. Alexandridis, B. Lindman, Macromolecules 30 (1997) 6788.

[36] K. S. W. Sing, D. H. Everett, R. A. W. Haul, L. Moscou, R. A. Pierotti, J. Rouquerol, T. Siemieniewska, IUPAC, Pure and Appl. Chem. 57 (1985) 603-619.

[37] J. Sun, H. Zhang, D. Ma, Y. Chen, X. Bao, A. Klein-Hoffmann,N. Pfaender, D.S. Su, Chem. Commun. (2005) 5343.

[38] H. Zhang, J. Sun, D. Ma, G. Weinberg, D. S. Su, X. Bao J. Phys. Chem. B 110 (2006), 25908.

[39] J.L. Blin, C. Otjacques, G. Herrier, B.L. Su, International J. Inorganic Mater. 3 (2001) 75.

[40] J.L. Blin, A. Léonard, B.L. Su, J. Phys. Chem. B 105 (2001), 6070.

[41] A. Galarneau, H. Cambon, F. Di Renzo, F. Fajula, Langmuir 17 (2001) 8328.

[42] M. Hartmann, A. Vinu, Langmuir 18 (2002) 8010.

[43] S.S. Kim, A. Karkamkar, T.J. Pinavaia, M. Kruk, M. Jaroniec, J. Phys. Chem. B 105 (2001), 7663.

[44] H. Zhang, J. Sun, D. Ma, X. Bao, A. Klein-Hoffmann, G. Weinberg, D. Su, R. Schlögl, J. Am. Chem. Soc. 126 (2004) 7440.

Published in: Microporous and Mesoporus Materials, Volume 169, 2013, Pages 235-241

Figure captions

Figure 1: ED900Myr/$C_{10}H_{22}$/water ternary system: composition phase diagram (wt %) at 20 °C.

Figure 2: ED900Myr/$C_{10}H_{22}$/water system: Hexagonal liquid crystal. **A**: value of the d_{100} reflection (d), **B**: hydrophobic radius (R_H) and **C**: cross-sectional area as a function of β(number of oil molecules per surfactant molecule) for various ED900Myr/water ratios (R). [○: R = 1; ▼: R = 1.47; ☆: R = 1.85 and ■: R = 2.31]. Lines in (A) are only a guide to the eye.

Figure 3: Porous materials: SAXS patterns (**A**) of the materials synthesized with a: 0, b: 1, c: 5 and d: 10 wt % of decane. Nitrogen adsorption-desorption isotherms (**B**) and pore size distribution (**C**) of materials prepared with ■: 0, ▽: 1, ▲ :5 and ○: 10 wt % of decane. The hydrothermal treatment has been performed at 50 °C during 44 hours.

Figure 4: Porous materials: **A**:SAXS patterns of samples synthesized with a: 0, b: 3, c: 5, d: 10, e: 20, f: 30, g: 50, h: 70 and i: 85 wt % of decane. **B**: Evolution of the nitrogen adsorption-desorption isotherm and the corresponding BJH pore size distribution curve (insert) with the concentration of decane a: 0, b: 3, c: 5, d: 10, e: 40 and f: 80 wt % of decane. The hydrothermal treatment has been performed at 80 °C during 24 hours.

Figure 5: Porous materials: Evolution of **A**: the d-spacing (d, ■), pore diameter (d_p, ○), the wall thickness (w_t, ●) and of **B**: the specific surface area with the decane concentration (wt %). The hydrothermal treatment has been performed at 80 °C during 24 hours. Lines are only a guide to the eye.

Figure 6: SEM micrograph of samples prepared with the concentration of decane a: 0; b: 7; c: 60; d and e: 80 wt .% of decane and TEM images of the materials

prepared with 80 wt % of decane (f-i). The hydrothermal treatment has been performed at 80 °C during 24 hours.

Published in: Microporous and Mesoporus Materials, Volume 169, 2013, Pages 235-241

Figure 1

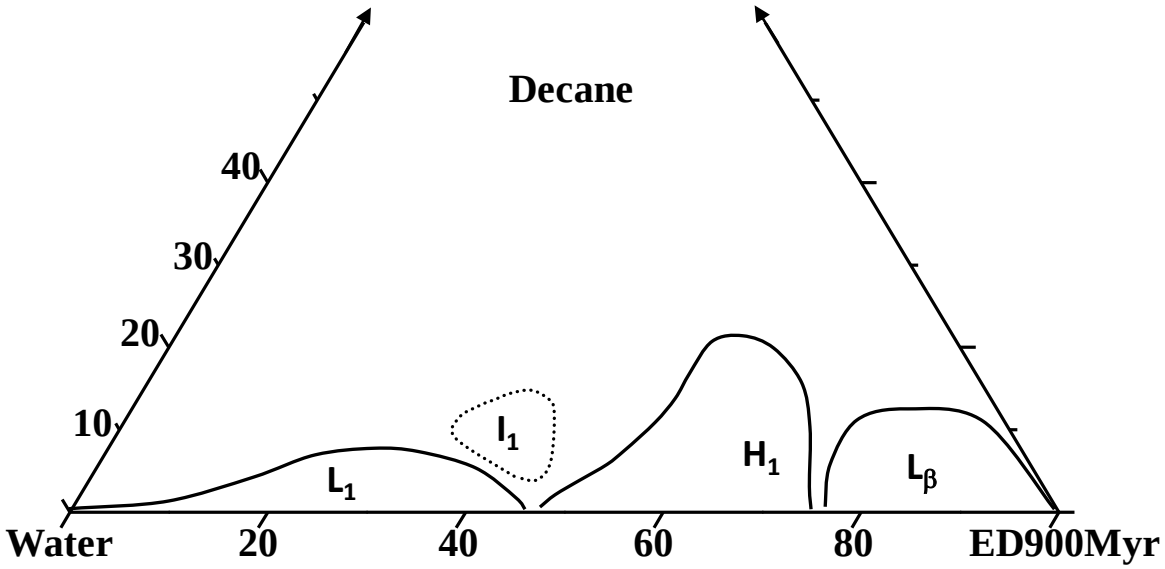

Published in: Microporous and Mesoporus Materials, Volume 169, 2013, Pages 235-241

Figure 2

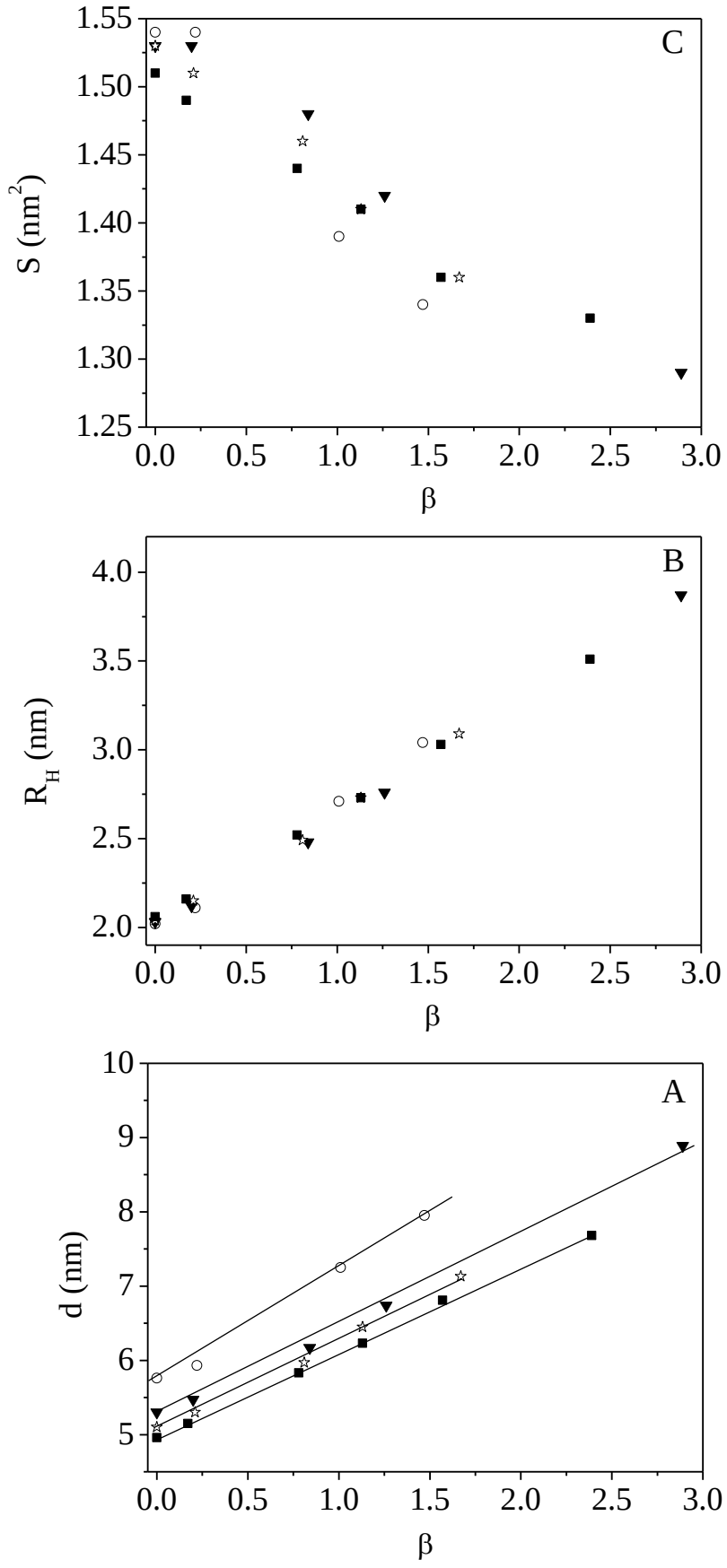

Published in: Microporous and Mesoporus Materials, Volume 169, 2013, Pages 235-241

Figure 3

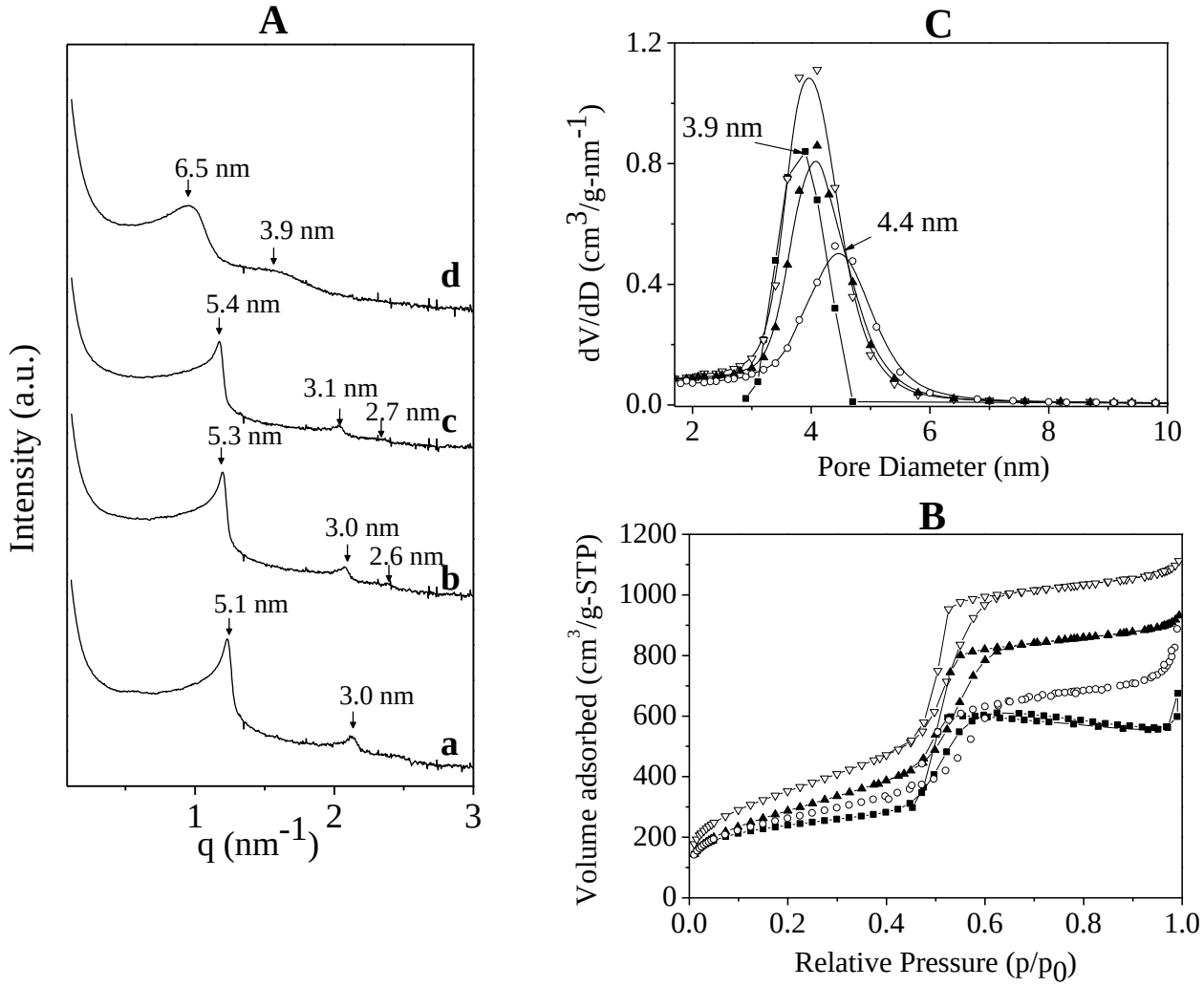

Published in: Microporous and Mesoporus Materials, Volume 169, 2013, Pages 235-241

Figure 4

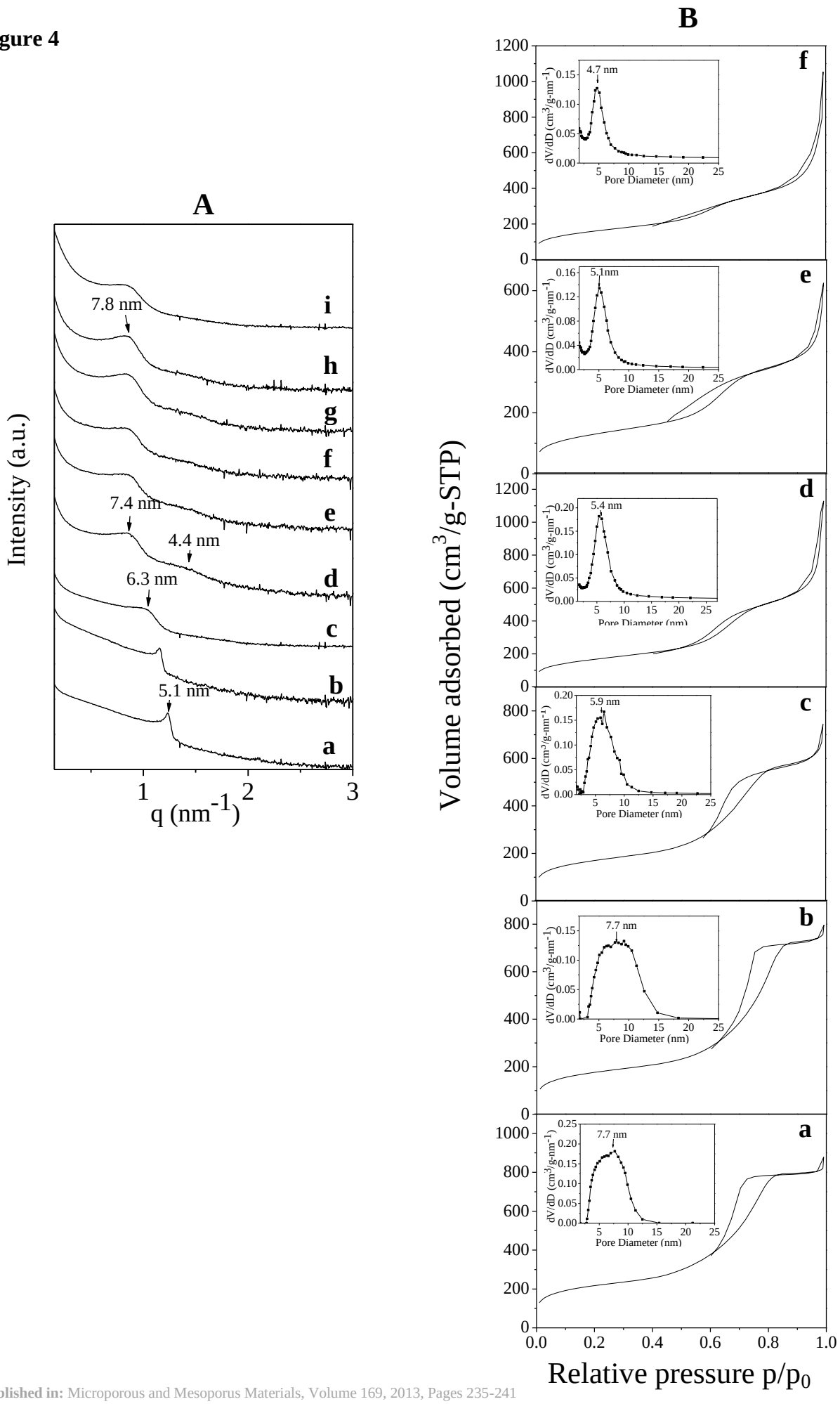

Published in: Microporous and Mesoporus Materials, Volume 169, 2013, Pages 235-241

Figure 5

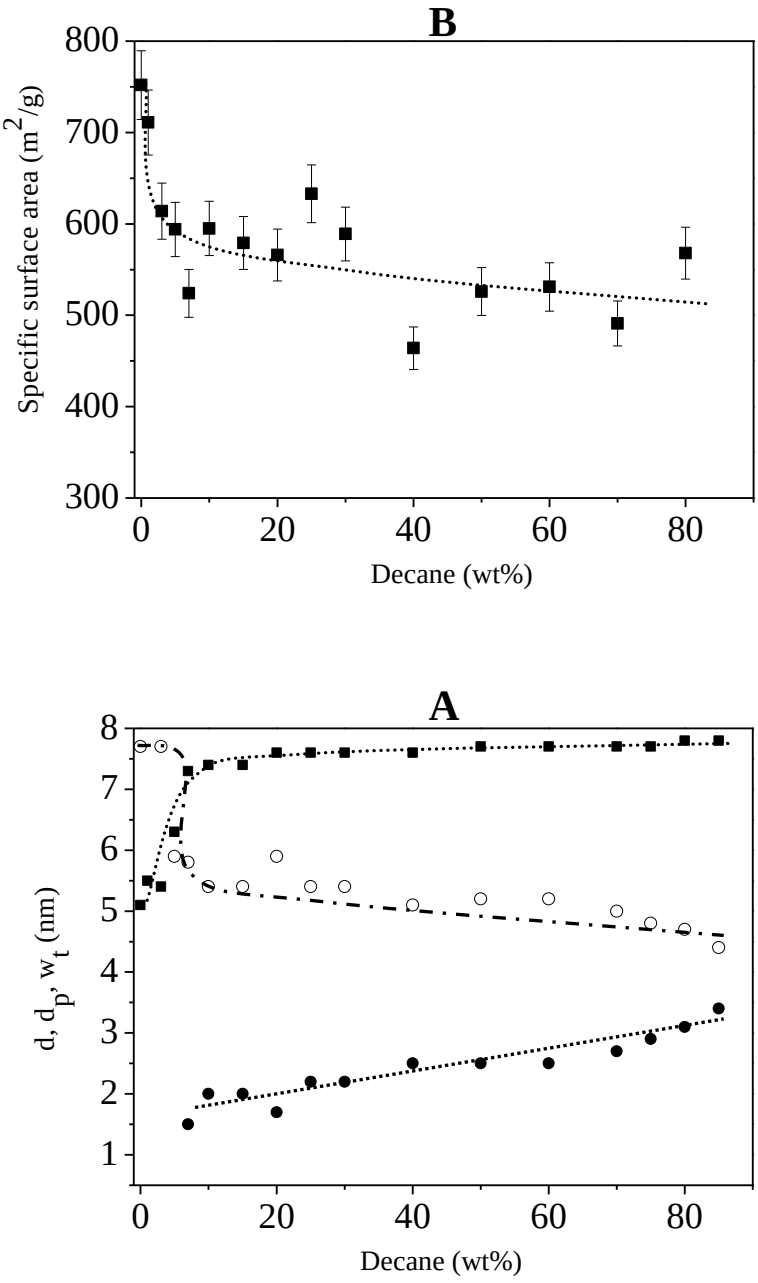

Published in: Microporous and Mesoporus Materials, Volume 169, 2013, Pages 235-241

Figure 6

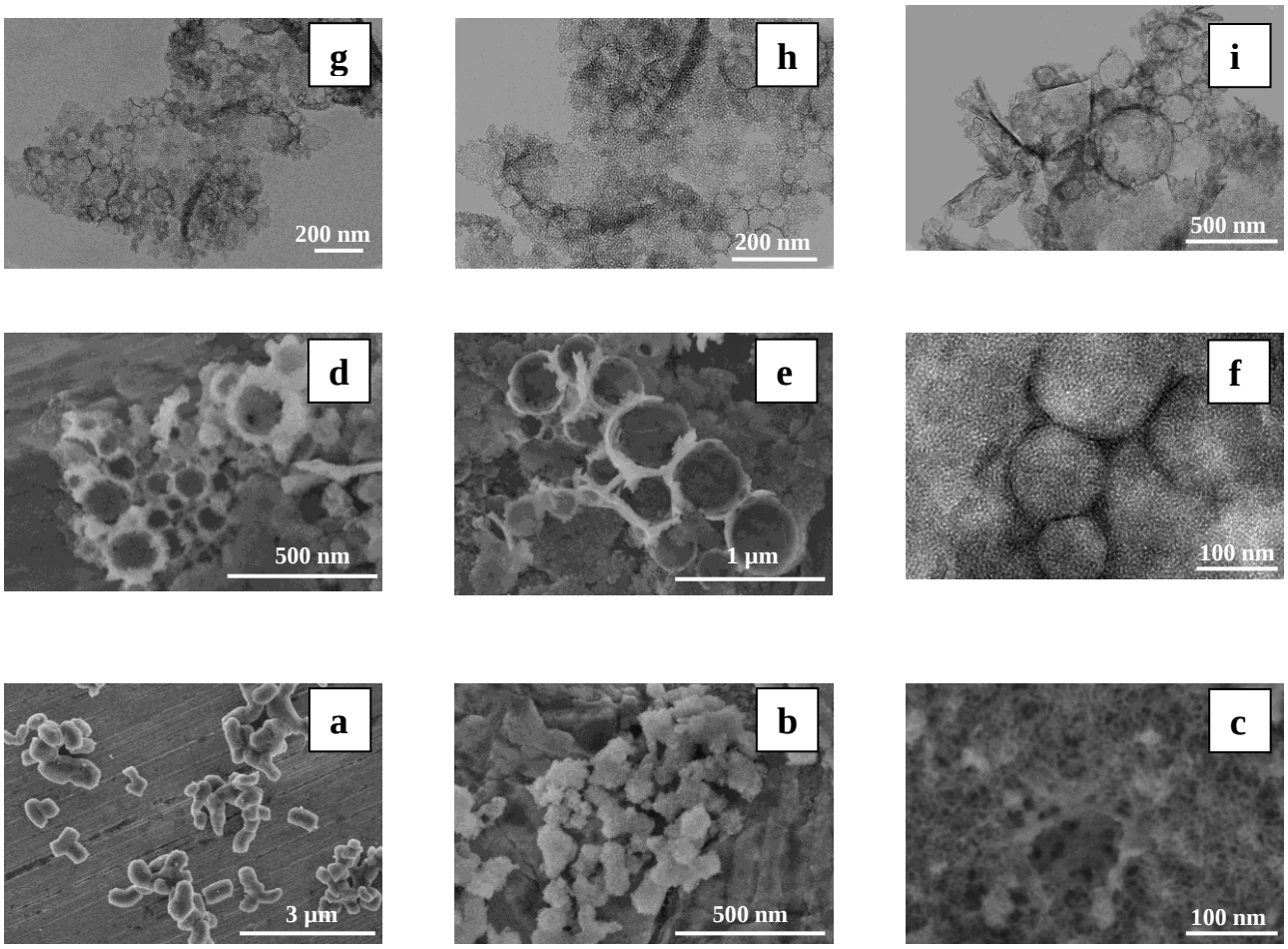

Published in: Microporous and Mesoporus Materials, Volume 169, 2013, Pages 235-241